Virology 514 (2018) 216–229

Contents lists available at ScienceDirect

Virology

journal homepage: www.elsevier.com/locate/virology

# The interplay between viperin antiviral activity, lipid droplets and Junín mammarenavirus multiplication

José R. Peña Cárcamo[a,1], María L. Morell[a,1], Cecilia A. Vázquez[b], Sezen Vatansever[c], Arunkumar S. Upadhyay[d,e], Anna K. Överby[d,e], Sandra M. Cordo[b,2], Cybele C. García[a,*,2]

[a] Laboratorio de Estrategias Antivirales, Departamento de Química Biológica (QB), Facultad de Ciencias Exactas y Naturales (FCEyN), Universidad de Buenos Aires (UBA)- Instituto de Química Biológica de la Facultad de Ciencias Exactas y Naturales (IQUIBICEN)-Consejo Nacional de Investigaciones Científicas y Técnicas (CONICET), Buenos Aires, Argentina
[b] Laboratorio de Bioquímica y Biología del virus Junín, QB, FCEyN, UBA-IQUIBICEN, CONICET, Argentina
[c] Graduate School of Science and Engineering, Koc University, Rumelifener Yolu, Istanbul, Sarıyer, Turkey
[d] Department of Clinical Microbiology, Virology, Umeå University, Umeå, Sweden
[e] Laboratory for Molecular Infection Medicine Sweden (MIMS), Umeå University, Umeå, Sweden

ARTICLE INFO

*Keywords:*
Junín virus
Viperin
Lipids droplets

ABSTRACT

Junín arenavirus infections are associated with high levels of interferons in both severe and fatal cases. Upon Junín virus (JUNV) infection a cell signaling cascade initiates, that ultimately attempts to limit viral replication and prevent infection progression through the expression of host antiviral proteins. The interferon stimulated gene (ISG) viperin has drawn our attention as it has been highlighted as an important antiviral protein against several viral infections. The studies of the mechanistic actions of viperin have described important functional domains relating its antiviral and immune-modulating actions through cellular lipid structures. In line with this, through silencing and overexpression approaches, we have identified viperin as an antiviral ISG against JUNV. In addition, we found that lipid droplet structures are modulated during JUNV infection, suggesting its relevance for proper virus multiplication. Furthermore, our confocal microscopy images, bioinformatics and functional results also revealed viperin-JUNV protein interactions that might be participating in this antiviral pathway at lipid droplet level. Altogether, these results will help to better understand the factors mediating innate immunity in arenavirus infection and may lead to the development of pharmacological agents that can boost their effectiveness thereby leading to new treatments for this viral disease.

## 1. Introduction

The *Arenaviridae* family includes viruses found in captive alethinophidian snakes (the reptarenaviruses) and viruses that circulate mostly in rodents (the mammarenaviruses) (Radoshitzky et al., 2015). The mammarenaviruses are divided into two groups -Old World and New World- based on their serology and geographic distribution. Seven mammarenaviruses can cause acute human viral hemorrhagic fever with high case fatality rates, including Junín virus (JUNV), the etiological agent of Argentine hemorrhagic fever (AHF) (Paessler and Walker, 2013). Although an effective live attenuated vaccine has been developed in Argentina to prevent AHF only in the endemic area, vaccination may not be a definitive solution to JUNV infection because of the emergence of new viral variants and no specific antiviral available against arenavirus infections (Enria et al., 2008). The exact mechanisms by which arenavirus cause its pathology still remain puzzling. The innate immune response has been widely accepted to be one of the essential factors that determine the outcome of arenavirus infection in patients; however other contributing factors might need to be considered. JUNV infections are associated with high levels of interferons

*Abbreviations:* G1, glycoprotein; IFN-I, type I interferon; ISGs, IFN stimulated genes; JUNV, Junín virus; LD, lipid droplets; MOI, multiplicity of infection; N, nucleocapsid protein; PFU, plaque forming unit; VIP, viperin

* Correspondence to: Laboratorio de Estrategias Antivirales, Departamento de Química Biológica, Facultad de Ciencias Exactas y Naturales, UBA, Ciudad Universitaria, Pabellón 2, Piso 4, 1428 CABA, Argentina.

*E-mail addresses:* jpena@qb.fcen.uba.ar (J.R. Peña Cárcamo), mlmorell@qb.fcen.uba.ar (M.L. Morell), cvazquez@qb.fcen.uba.ar (C.A. Vázquez), svatansever13@ku.edu.tr (S. Vatansever), upadhyay.arunkumar@umu.se (A.S. Upadhyay), anna.overby@umu.se (A.K. Överby), scordo@qb.fcen.uba.ar (S.M. Cordo), cygarcia@qb.fcen.uba.ar (C.C. García).

[1] J.R. Peña Cárcamo and M.L. Morell contributed equally to this work.

[2] S.M. Cordo and C.C. García are equally responsible senior authors.

https://doi.org/10.1016/j.virol.2017.10.012
Received 19 January 2017; Received in revised form 10 October 2017; Accepted 12 October 2017
Available online 01 December 2017
0042-6822/ © 2017 Elsevier Inc. All rights reserved.

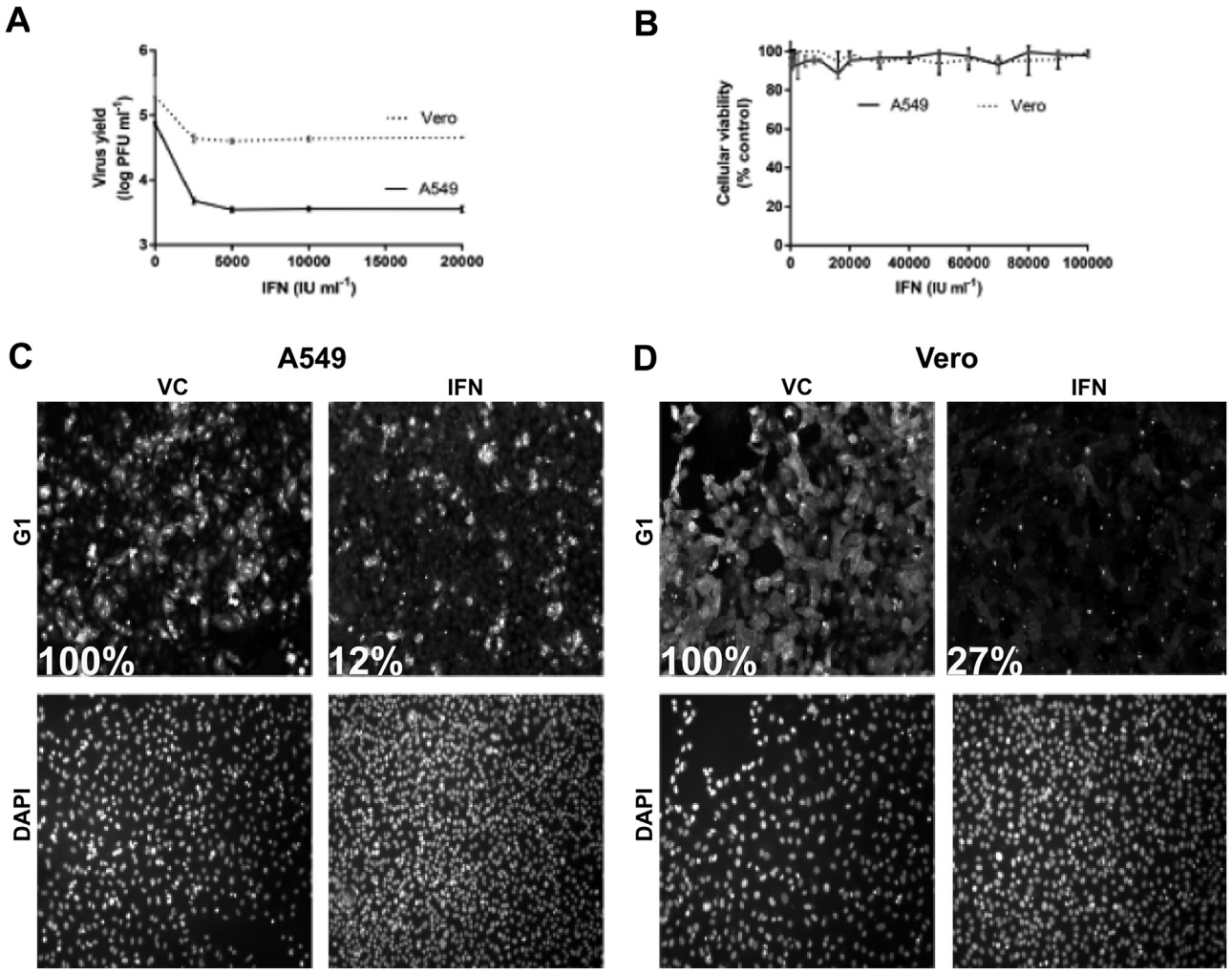


**Fig. 1. JUNV sensitivity to IFN treatment.** (A) Cell cultures were pre-treated with IFN (0–100000 IU/ml) for 8 h and then infected with JUNV at MOI of 0.1 PFU/cell. Virus yield was quantified from cell supernatants at 24 h p.i. (B) Cell viability upon IFN treatment was determined in each cell line by MTT assay. After IFN treatment (2000 IU), viral G1 protein expression was determined at 24 h p.i. in A549 (C) and Vero infected cells (D). Depicted percentages represent quantification of G1 positive cells over total cells. DAPI staining shows the corresponding cell nuclei for each image. Magnification: 100×.

in both severe and fatal cases (Levis et al., 1984). Accordingly, in vitro infection of several cell types by different arenaviruses have been shown to induce type I interferon (IFN-I) (Huang et al., 2014, 2015; Pythoud et al., 2015). The Arenaviruses genome is composed of two single-stranded molecules of RNA called L (ca 7.1 kb) and S (ca 3.4 kb), both exhibiting an ambisense coding strategy. The S segment encodes the nucleoprotein (N) and the envelope glycoprotein precursor (GPC). GPC is processed post-translationally yielding a mature glycoprotein complex formed by three subunits that remain non-covalently linked: the signal peptide SSP, the external receptor-binding G1 protein and the transmembrane fusion G2 protein (Eichler et al., 2003; York et al., 2004). The L segment encodes the RNA-dependent RNA polymerase L and a small protein called Z. So far, two arenavirus proteins have been reported as modulators of the IFN-I response: N and Z. Regarding N, it has been reported that Old World lymphocytic choriomeningitis arenavirus (LCMV) N negatively modulates IFN production in persistently infected A549 cells by inhibiting nuclear translocation of the interferon regulatory factor 3. This property has also been demonstrated for the N protein of several representatives of the Old and New World mammarenaviruses, including JUNV (Martínez-Sobrido et al., 2006). On the other hand, Z protein from pathogenic New World arenaviruses antagonizes IFN response by binding to the retinoic acid-inducible gene I (RIG-I) and inhibiting downstream activation of IFN-I expression signaling pathway (Fan et al., 2010; Xing et al., 2015). From many of these studies it can be concluded that viral modulation of the IFN response is a key event that determines mammarenavirus pathogenicity. However, a comprehensive characterization of IFN stimulated genes (ISGs) involved in the innate immune response against mammarenavirus infection is still missing.

Viperin, encoded by an ISG, is a highly conserved 361-amino-acid protein, with a predicted molecular weight of 42 kDa. It was first identified as a human cytomegalovirus (HCMV)-inducible gene in fibroblasts (Chin and Cresswell, 2001). This protein harbors an amphipathic α-helix domain at its N-terminus that serves as an anchor to lipid membranes. Viperin localizes in the endoplasmic reticulum (ER) from which it is transported to lipid-enriched compartments called lipid droplets (LDs) (Wang et al., 2013). LDs are intracellular sites for neutral lipid storage and are critical for lipid metabolism and energy homeostasis. In immunity, new roles for LDs have been uncovered, with evidence that they act as assembly and replication platforms for specific viruses and as reservoirs for proteins that counteract intracellular pathogens (Jiang and Chen, 2011; Saka and Valdivia, 2012). It has also been demonstrated that viperin is able to bind and inhibit the farnesyl pyrophosphate synthase (FPPS), an enzyme involved in the synthesis of multiple isoprenoid-derived lipids (Makins et al., 2016). Thus, cholesterol-rich rafts membranes that serve as sites for recruitment of several viral proteins are consequently perturbed, and virus release impaired (Wang et al., 2007).

JUNV is an enveloped virus that has been shown to rely on specific cellular lipid configuration. Data from our earlier studies showed that treatments altering general lipid metabolism diminished virus yield suggesting an intimate relationship between viral morphogenesis and lipid availability (Cordo et al., 1999). More recently it has also been demonstrated that cholesterol enriched membrane microdomains are involved in proper JUNV budding and infectious particle production (Cordo et al., 2013; Gaudin and Barteneva, 2015). Novel cellular lipid structures are constantly being characterized, and their participation in JUNV lipid-dependent multiplication remains to be evaluated. This work intends to extend knowledge on cellular antiviral factors focusing on lipid structures that are of great importance for virus replication and a putative place for interplay between viperin and JUNV proteins.

## 2. Results

### 2.1. JUNV sensitivity to IFN treatment

Reports addressing the effect of IFN treatment over pathogenic and non-pathogenic mammarenaviruses like JUNV, Machupo and Tacaribe viruses arrived to a variety of conclusions ranging from a modest to a high sensitivity to IFN treatment (Huang et al., 2015, 2012; Groseth et al., 2011). However, those studies were performed in different cell lines from different origins (mouse and human) and also different JUNV strains have been used. For this reason, we sought to determine the IFN sensitivity degree in our model of study, A549 cells, in order to relate it to further viperin anti-JUNV functions. To test this, we decided to use also Vero cells where IFN pathway is deficient. Thus, A549 and Vero cell cultures were pretreated with a range of IFN concentrations, then infected at a MOI of 0.1 PFU/cell, and virus extracellular production was measured at 24 h post infection (p.i.). As can be seen in Fig. 1A, both cell lines were permissive to JUNV infection, although virus yield was significantly higher in Vero IFN deficient cell line compared to A549 IFN competent cell line. Noticeably, viral production was reduced by 1 log in the presence of IFN in both cell models, confirming JUNV sensitivity to cell IFN pretreatment.

Further treatments with higher IFN concentrations showed similar reduction on virus production, suggesting that IFN effect over JUNV multiplication was already established in these cell cultures and reached its maximum in these systems. The IFN concentrations used in the assays 2000–100000 IU/ml) were compatible with cell viability (Fig. 1B), so decreased viral production was specific. Microphotographs on Fig. 1C-D showed that number of A549 and Vero infected cells was reduced by IFN treatment by an 88% and 73%, respectively. In conclusion, A549 and Vero cell cultures were able to respond to IFN treatment and this response impaired JUNV multiplication.

### 2.2. Endogenous viperin is upregulated upon JUNV infection

Viperin induction through classical IFN pathways has been previously demonstrated (Hinson et al., 2010; Seo et al., 2011; Helbig and Beard, 2014). As a primary approach to study the role of any putative restriction factor we decided to quantify levels of important mRNAs of the IFN-I pathway. Expression of RIG-I, TLR3, MYD88, TRAF6 and IL6 mRNAs after IFN treatment was analyzed by real time PCR (Fig. 2A). mRNA levels corresponding to the dsRNA sensor receptor molecules RIG-I and TLR3 were upregulated, reaching a 4.95 ± 0.3 and 2.9 ± 0.3-fold increase, respectively, in relation to non-treated cells at 24 h. On the other hand, TRAF6, MYD88 and IL6 analyzed mRNA did not show any fold change in this condition. Then, we studied viperin mRNA levels at different time points after IFN treatment. As it is shown in Fig. 2B, no differences in viperin mRNA abundance with respect to non-treated cell cultures were found at 8 h after treatment. However, sustained rising viperin mRNA levels reaching a 2.7 ± 0.3 change fold were observed at 24 h, and similar values were observed at 48 h after IFN treatment (Fig. 2B). Although with higher values along all analyzed time points, the upregulation of the pathogen sensor RIG-I was similar to viperin kinetics (data not shown) supporting that the IFN pathway was specifically induced. Then, we evaluated this specific activation profile upon JUNV infection. A549 cells were infected at a MOI of 0.1 PFU/cell and mRNA levels were determined at 48 h p.i. All cellular mRNAs studied were found upregulated in infected cell cultures (Fig. 2C). In addition, viperin expression showed a 22.2 ± 3 fold increment, while viral Z mRNAs level reached an 80.64 ± 7 fold change (Fig. 2D). Overall these results indicated that actively replicating virus effectively induced the antiviral response in these cells. In order to confirm this observation, we infected cells previously induced to an antiviral state by IFN treatment. Alternatively, we also infected A549 cells with a UV-JUNV treated stock. Reduced levels of JUNV Z mRNA upon IFN treatment, together with a modest up-regulation of viperin mRNA were measured. As expected, no Z mRNA was detected and viperin mRNA was not found upregulated in cultures infected with inactivated particles. Finally, we also infected A549 cells previously transfected with viperin-siRNAs. We did not find detectable viperin mRNA levels but importantly a significant 804 ± 89 fold upregulated Z mRNAs expression in viperin silenced cultures compared to 80 fold increase in infected cells (Fig. 2D).

### 2.3. Viperin expression along JUNV infection

Since important upregulation of viperin mRNA was confirmed in A549 cells infected by replicative competent JUNV stock, we sought to better delineate kinetics of both viperin expression and viral replication. For this, infected cultures were analyzed at different times p.i. as results depicted in Fig. 3. JUNV replication was monitored by means of Z mRNA levels showing a 15 ± 0.1 fold increment at 10 h. p.i. and followed by a continuous raising up to a 60 ± 4 fold increase at 48 h p.i. (Fig. 3A). With the same tendency it is worthy to note that while at 6 h p.i. viperin mRNA levels were increased to 2–3 fold change; at 24 h p.i its abundance was remarkably higher with an increment of 15 ± 2-fold change (Fig. 3A).

In order to study viperin protein expression, we performed immunofluorescence assays and found that endogenous viperin is not detected at early times p.i. (ranging from 0 to 10 h p.i.) in JUNV-infected cells (Fig. 3B). However, after 24 h p.i. viperin expression was observed in a cytosolic punctate-diffuse pattern as reported (Chin and Cresswell, 2001). This expression was detected after a considerable accumulation of viral RNA (Fig. 3A) and glycoprotein expression (Fig. 3C), indicating that this host restriction factor is stimulated upon JUNV replication. Noticeably, we found that viperin expression diminished at 48 h p.i (Fig. 3C). Together these results strongly suggest that viperin may play a role in controlling natural JUNV infection.

### 2.4. Viperin overexpression has a strong antiviral action against JUNV

Importantly, and for the first time, our experiments showed that endogenous viperin is upregulated upon JUNV infection. Viperin is expressed in most cell types at very low basal levels, thus most of the work characterizing its antiviral activity is done using viperin encoding plasmids (Tan et al., 2012; Teng et al., 2012; McGillivary et al., 2013). Hence, we decided to explore the effect of enhanced viperin action upon JUNV multiplication by an overexpression approach. Viperin transfected A549 cells were infected at a MOI of 0.1 PFU/cell. Also, empty vector transfected cells were infected and included as viral controls. Supernatants were harvested at 24 h p.i. to determine virus yields and at the same time cells were fixed to analyze viral antigen expression by immunofluorescence. Extracellular viral production was remarkably reduced in viperin overexpressing cell cultures as reflected by the 1.5 ± 0.1 log decrease in JUNV yield (93%), measured by standard plaque assay (Fig. 4A). Moreover, a significant reduction in number of G1 expressing cells was observed. Interestingly, source of this reduction corresponded to number of G1 positive cells per viral

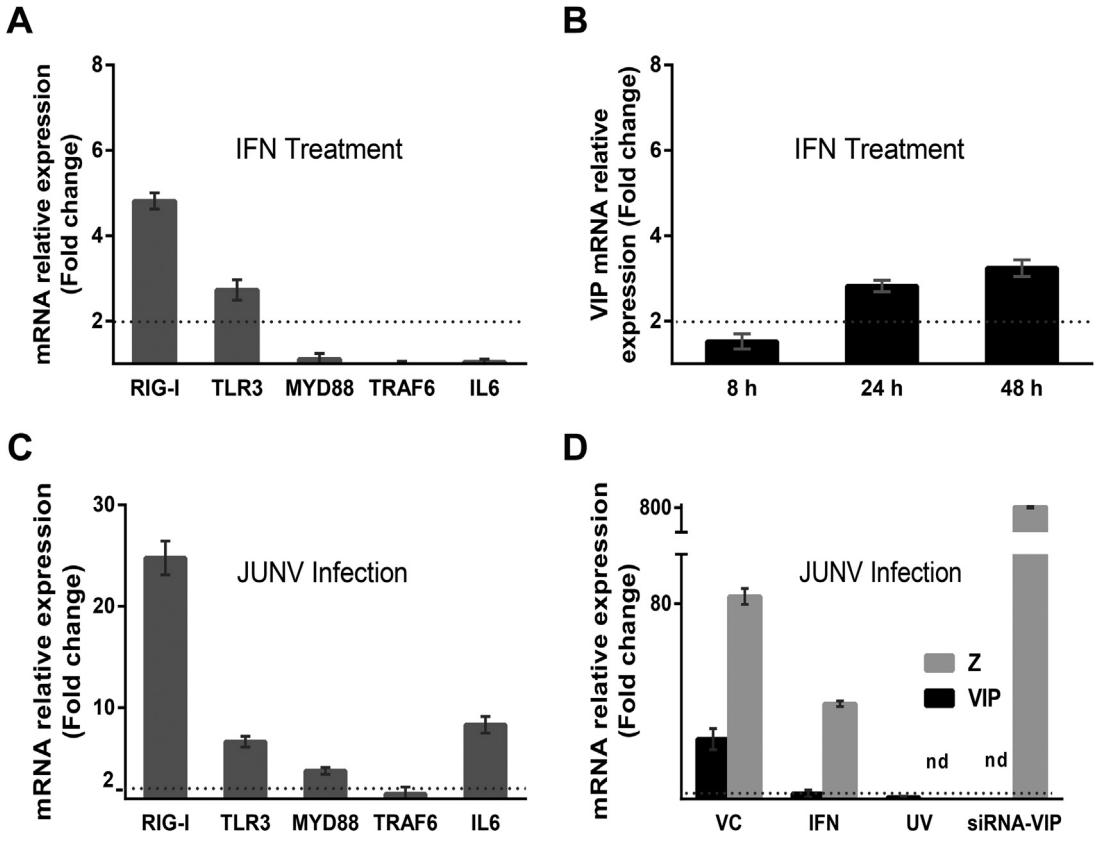


**Fig. 2. Differential levels of mRNAs in A549 cells after IFN treatment or JUNV infection.** (A) A549 cells were pre-treated with 10,000 IU/ml of IFN-I for 8 h or (C) infected with JUNV, and 24 h later, expression of RIG-I, TLR3, MYD88, TRAF6 and IL6 genes was determined. (B) Viperin mRNA levels determination was performed at 8, 24 and 48 h post IFN treatment. (D) Relative levels of viperin mRNA and sum of Z mRNA and viral L genomic RNA were determined at 48 h p.i. in: JUNV infected cells (VC), JUNV infected IFN pre-treated cells (IFN), UV-inactivated JUNV infected cells (UV) or previously transfected with viperin-siRNAs JUNV infected cells (siRNA-VIP). All mRNA determinations were performed by qRT-PCR. mRNA levels were normalized to β-actin-mRNA and represented as fold difference with respect to controls with a threshold value set on 2 (dotted line). nd: non detectable levels of mRNA of Z. In all experiments viral titers were $5 \times 10^5 - 1 \times 10^6$PFU/ml.

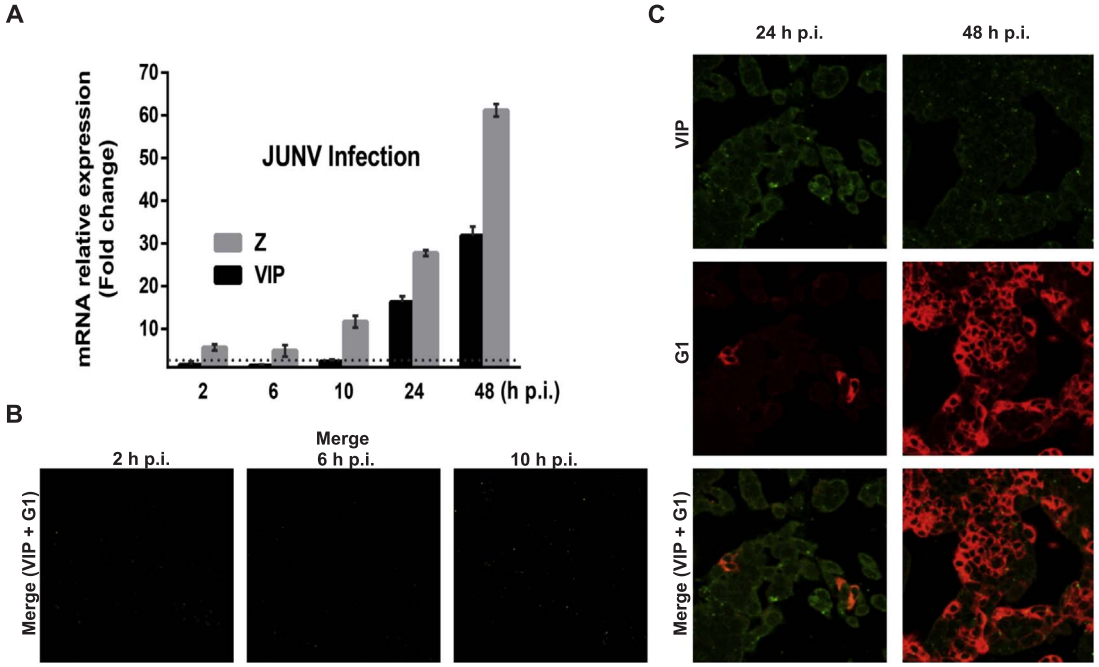


**Fig. 3. Endogenous viperin expression along infection progression.** (A) A549 cells were infected with JUNV at MOI of 0.1 PFU/cell. Viperin and Z mRNA levels were measured by qRT-PCR at 2, 6, 10, 24 and 48 h p.i. (B) Kinetics of endogenous viperin and G1 protein expression were revealed by immunostaining with rabbit polyclonal anti-viperin and mouse monoclonal anti-G1 antibodies at 2, 6, 10, 24 and 48 h p.i. Magnification: 400×.

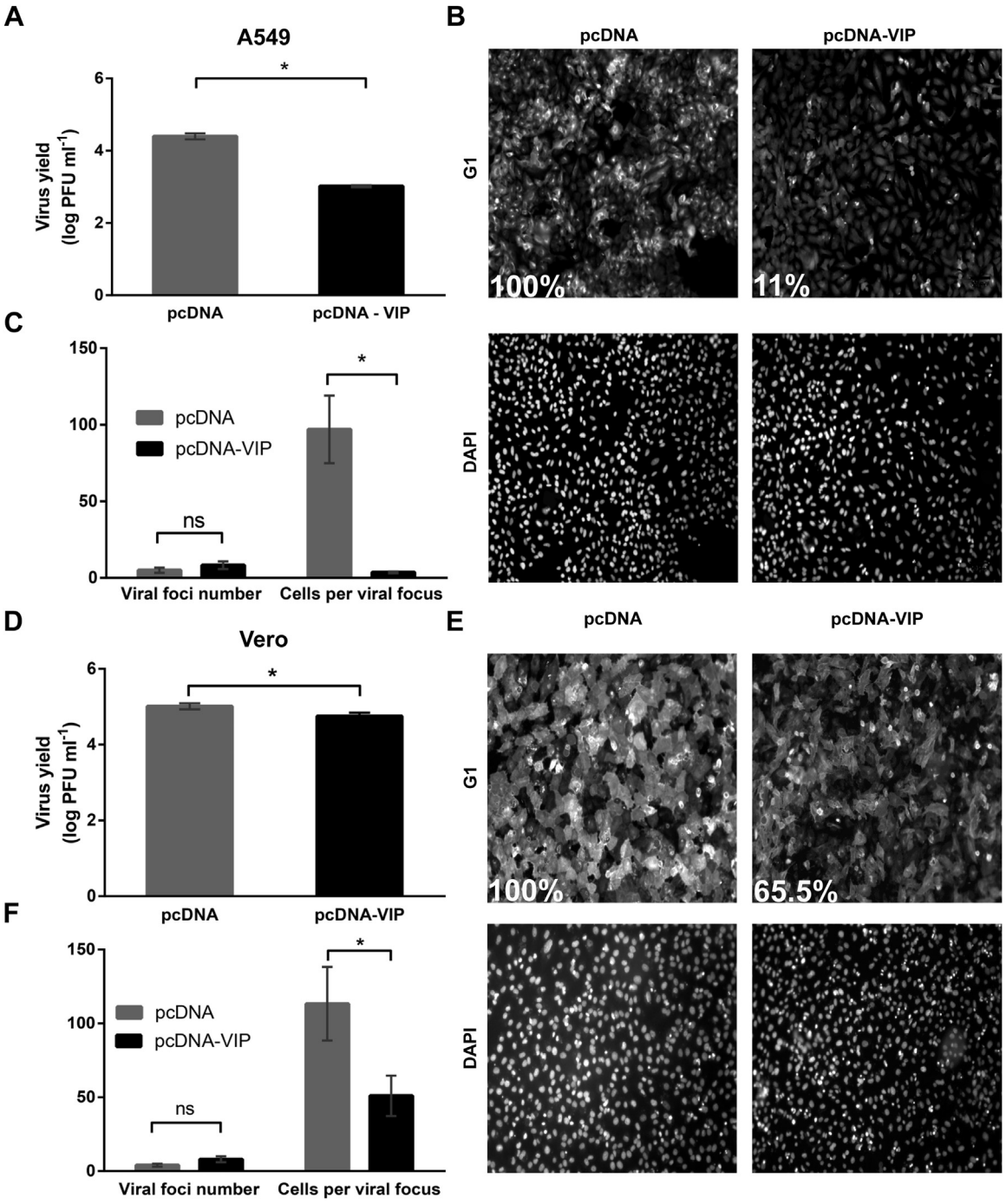


**Fig. 4. Effect of viperin overexpression on JUNV multiplication.** A549 (A-C) or Vero (D-F) cells were transfected with empty pcDNA 3.1 or pcDNA 3.1 viperin encoding vector and infected with JUNV at MOI of 0.1 PFU/cell. At 24 h. p.i. viral yields were determined by a standard plaque assay (A and D). Reported values are mean ± SD (n = 2). At 24 h p.i. cells were fixed and total viral glycoproteins were stained using mouse monoclonal anti-G1 antibodies and Alexa 568-conjugated goat anti-mouse IgG (B and E). Cell nuclei were stained with DAPI. Samples were visualized by epifluorescence microscopy. Magnification: 100X. Quantification of number and size of viral foci (C and F) corresponds to images in B and E. ns: non significative. (*) significative values.

focus rather than number of viral foci, when comparing empty vector to viperin overexpressing A549 cell cultures (Fig. 4B). Detailed inspection under the microscope showed that while viral foci containing 91 infected cells in average were seen in viral control, only 3 cells per viral focus in average were detected in presence of overexpressed viperin (Fig. 4C). These results suggested that although the first round of infection was successfully achieved, impairment in viral propagation could take place in viperin overexpressing cultures. To further test antiviral function of viperin, IFN deficient Vero cells were transfected with viperin encoding plasmid as in experiments described above and both viral production and level of viral protein expression were quantified. Fig. 4D-F shows that exogenous expression of viperin turned the cultures less permissive to JUNV propagation confirming once again viperin as a genuine antiviral candidate.

### 2.5. Viperin overexpression results in mislocalized viral glycoproteins

Experiments above showed that neither entry nor glycoprotein synthesis were affected in overexpression conditions. However, infectious virus release was significantly inhibited by viperin

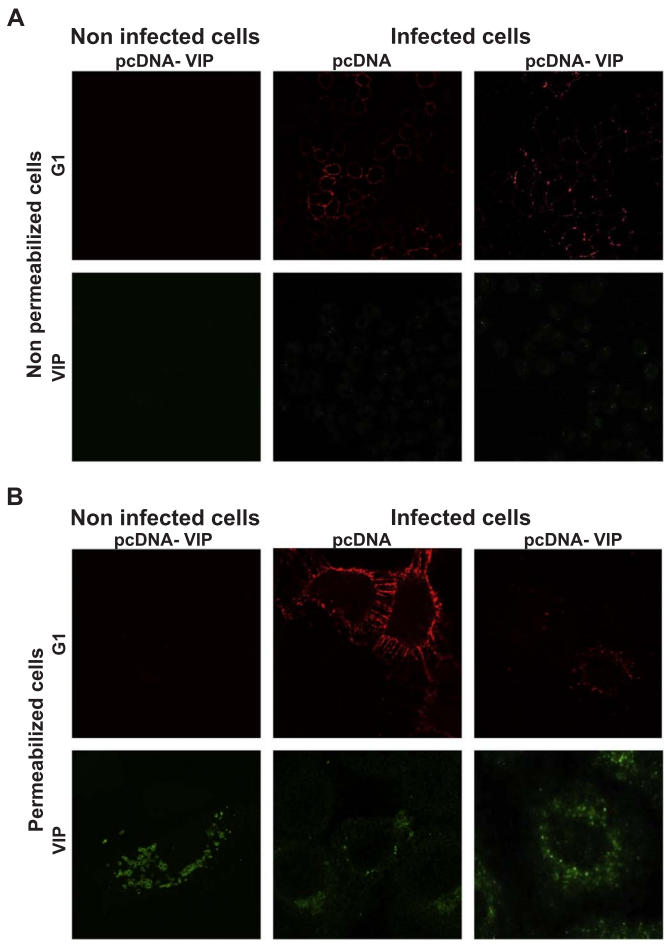


**Fig. 5. Viperin overexpression results in mislocalized viral glycoproteins.** Empty vector or viperin encoding vector transfected A549 cells were infected with JUNV, incubated with mouse monoclonal anti-G1 or anti-viperin antibodies and fixed. Non permeabilized (A) and permeabilized (B) cell cultures were stained with secondary antibodies and visualized with a confocal microscope as indicated in Materials and methods. Magnification: (A) 400×; (B) 600×.

overexpression (Fig. 4A). JUNV particle production and propagation depends on proper insertion of glycoproteins into cellular membranes. Thus, a reduced membrane glycoprotein expression might be a possible explanation for this observation. To assess that, viperin overexpressing cultures were infected and then fixed without further permeabilization steps. Samples were revealed by immunofluorescence and analyzed by confocal microscopy. As can be seen in Fig. 5A, in JUNV infected cells viral G1 expression was in accordance with membrane pattern localization and defined ring-like structures are observed on those infected cells, as expected. On the other hand, viperin overexpressing-infected cells showed diminished G1 membrane localization and a surface discontinuous pattern. In addition, when samples were revealed with anti-viperin antibodies, it was confirmed that viperin does not localize on the cell surface. Another set of samples were analyzed including a membrane permeabilization step. Fig. 5B showed that in JUNV infected cells, G1 expression was continuous along cell membrane and depicted long filaments. However, in accordance with Fig. 5A, this G1 pattern was observed completely altered in viperin overexpressing-JUNV infected cells (Fig. 5B). Finally, another important observation was that viperin overexpression was detected as strong drop-like structures close to and around the nucleus but also at cellular periphery. Surprisingly, in those infected viperin-transfected cells the drop-like structure switched to a punctate diffuse pattern (Fig. 5B).

### 2.6. Interplay of viperin and LDs during JUNV infection

There is a known relationship between viperin and LDs (Hinson and Cresswell, 2009a). In addition to cytosolic LDs that are present in most other cell types, hepatocytes contain at least two more types of LDs in the lumen of the ER where viperin is localized. Therefore, we included HepG2 cells to study the interplay between viperin and LD during JUNV infection. First, in order to confirm IFN pathway activation upon JUNV HepG2 cell line infection, we measured RIG-I and viperin mRNA levels. At 24 and 48 h p.i. both mRNAs were found upregulated (Fig. 6A). Then, non-infected and JUNV-infected HepG2 cells were fixed and these lipid cellular structures were identified and enumerated by perilipin 2 (Plin 2) staining. Representative images are shown in Fig. 6B. Values from this analysis indicated that number of LDs is significantly decreased upon JUNV infection when comparing to non-infected -JUNV negative- cells (Fig. 6C).

Decreased LDs content in JUNV-infected cells lead us to the hypothesis that these cellular structures are important for proper viral multiplication. To test this hypothesis, we used the compound C75 which reduces the amount of LDs in cells (Ronnett et al., 2005) and inhibits pre-adipocyte differentiation (Loftus et al., 2000; Kuhajda et al., 2005). First, we investigated viability of HepG2 cells after incubation with different C75 concentrations. As can be seen in Fig. 7A, after incubation of cell cultures with up to 23 μM C75 non-important cytotoxic effects were detected by two different methods. Noticeably, the concentration of 23 μM reduced LD staining by 47.5% (Fig. 7B). Then, to discard any possible direct effect of C75 on virion infectivity, the virus suspension was incubated with different compound concentrations and remaining infectivity was determined by plaque assay. Pre-incubation of the virus suspension with C75 did not produce any inhibition in virus yield (Fig. 7C). Lastly, HepG2 cells were infected then treated with C75 and extracellular virus production was quantified by plaque assays at 48 h p.i. In Fig. 7D it is shown that viral production was significantly diminished when LDs morphogenesis was blocked. This virus yield inhibition occurred in a dose dependent manner with a maximum inhibition of 2 ± 0.1 logs relative to viral control yields.

At present, the role of LD on JUNV infection remains unexplored. Consequently, we investigated whether JUNV proteins localized near these structures. In order to inspect that possibility, JUNV-HepG2 infected cells were immunostained with mouse monoclonal specific antibodies to detect major viral proteins (G1 and N) and probed with BODIPY for LD identification. As is shown in Fig. 8A, no significant correlation was seen with LDs while studying G1 localization. However, confocal microscopy images showed several co-localization spots between N and LD (Fig. 8B).

### 2.7. JUNV-viperin interaction studies

In order to have an overall picture of viperin and all viral proteins localization, immunofluorescence assays were performed using a polyclonal antiserum against whole JUNV antigens. Noticeably, confocal double staining microscopy images showed immuno-colocalization of viperin and JUNV proteins (Fig. 9A). Several reports indicate that viperin inhibits viruses by localizing to LDs. Results in Fig. 8B showed that N might localize at these subcellular structures, thus this protein could be a primary candidate for interacting with viperin. Then, immunoprecipitation assays were performed with JUNV infected samples at 24 and 48 h p.i. Antibodies recognizing N protein were incubated with infected cell lysates followed by protein A-agarose precipitation and extensive washes the samples were probed with anti-viperin antibodies. Fig. 9B showed that anti-N immunoprecipitation was able to pull-down endogenous viperin in the infected cell lysates. Control cultures showed no reactivity as expected.

In order to further analyze this N-viperin interaction, A549 cells were co-transfected with N and viperin encoding plasmids. At 24 h post transfection (p.t.), cells cultures were fixed and stained with specific

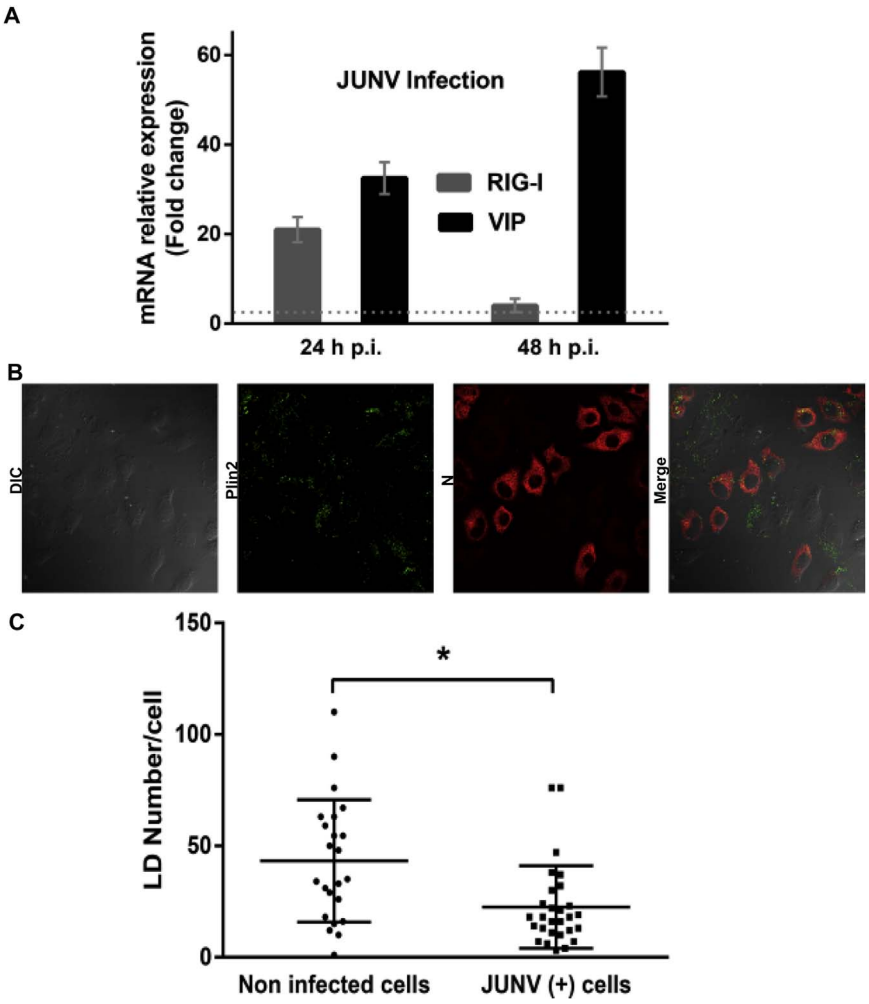


**Fig. 6. LD characterization in JUNV infected HepG2 cells.** (A) HepG2 cells were infected at MOI of 0.1 PFU/cell and expression of RIG-I and viperin genes was determined at 24 h and 48 h p.i. (B) Control uninfected and JUNV infected HepG2 cultures were fixed and probed for LDs detection and viral G1 viral antigen. Representative images of cultures probed with Plin2 (green channel) and G1 (red channel). (C) LDs quantification of JUNV (+) cells over negative cells. Brightfield and merge of all channels are also shown. Magnification 600X. ns: non significative. (*) significative values.

antibodies to assess co-localization of these proteins. As can be seen in Fig. 9C (merge panel), yellow spots corresponded to overlap proteins patterns. Further detailed analysis of confocal images demonstrated co-localization of N and viperin signal, with a Pearson coefficient of 0.65 (Fig. 9C). Next, HEK 293 cells were co-transfected with Flag-tagged viperin and HA-tagged N protein encoding plasmids. Cell lysates were subjected to anti-Flag or anti-HA immunoprecipitation and immunoprecipitated proteins were analyzed by immunobloting using anti-tag antibodies. As can be seen in Fig. 9D, regardless of antibodies used to pull down protein complexes, both tagged proteins were detected in the immunoprecipitated samples, supporting that N and viperin are interacting.

These results led us to address the specific residue interaction sites by bioinformatic modelling analysis. We investigated N and viperin interaction by using protein-protein docking tools in a comparative manner. We obtained N-viperin protein complex structure and the resulting model showed that C-terminal domain of JUNV N protein would interact with viperin (Fig. 10A). In particular, the first group of predicted interactions was between α4 and β5 residues of N and α4 residues of viperin (aa 186–215); the second group was between α5 and α6 residues of N and α3 residues of viperin (aa 164–170), depicted as discontinuous lines in zoomed Fig. 10A. These predicted interactions supporting results showed in Fig. 9 were confirmed with the aid of viperin protein mutant domains depicted in Fig. 10B. Co-immunoprecipitation analyzes using a viperin-specific antibody showed that all used mutants still interacted with N but TN50 mutant (Fig. 10C). This indicates that the presence of N-terminus of viperin is a necessary requirement for the protein-protein complex formation.

Jointly, these data showing viperin-N interaction suggested that JUNV N functionality may be hampered by this restriction factor. Since arenavirus replication-transcription complexes (RTC) are nucleated by the N, viperin might be interacting with this viral ribonucleoprotein in order to counteract its function on genome viral transcription/replication. To explore this hypothesis, we specifically measured RNA transcription process using appropriate primers (García et al., 2009). Viral mRNA level after 8 h p.i. was quantified in presence or absence of overexpressed viperin. As it can be seen in Fig. 10D, viral mRNA levels were significantly inhibited in viperin transfected- JUNV infected cell cultures.

Altogether, these results showed that viperin is antivirally active against JUNV and that it interacts with JUNV N protein as tested in co-immunoprecipitation, co-transfection and *in silico* assays. This interaction might be affecting the essential role of N in RNA transcription/replication, possibly at a LD subcellular level.

## 3. Discussion

Study of host-viral interactions has recently uncovered a number of restriction factors and has been extremely enlightening for the field of intrinsic immunity as well as for molecular biology (Kluge et al., 2015). Viral modulation of proteins involved in the IFN response is a key event that could help to explain mammarenavirus pathogenicity. Here we report for the first time that viperin is an important antiviral factor against JUNV infection.

In the present work, we showed that JUNV is able to replicate in IFN competent cell lines (Fig. 1), although the production of the viral RNA

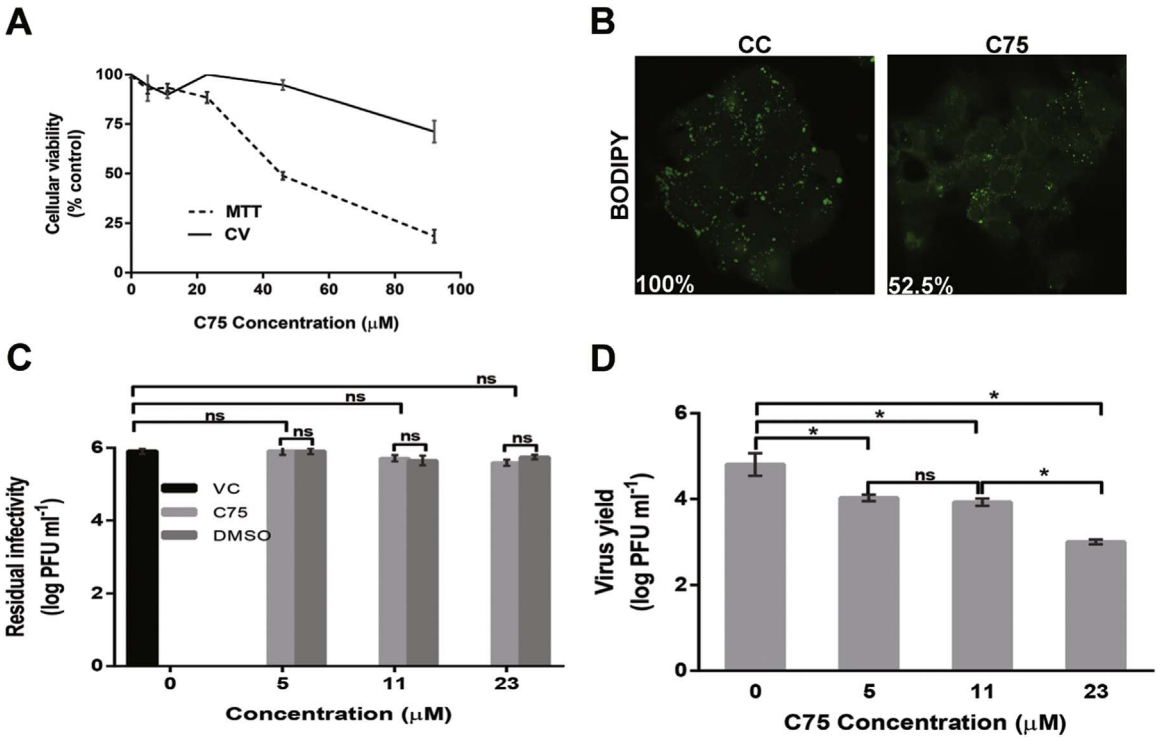


**Fig. 7. Effect of C75 on JUNV multiplication.** (A) HepG2 cells were incubated for 48 h with different concentrations of C75 and then cell viability was determined by MTT and crystal violet assays. (B) Untreated (CC) and 23 μM C75 treated HepG2 cells were fixed and probed with BODIPY. LD abundance was quantified as explained in Materials and methods. Magnification: 600X. (C) JUNV suspensions were incubated with increasing concentrations of C75 and remaining JUNV infectivity was determined by plaque assay. (D) JUNV infected cultures were incubated in presence or absence of C75 and virus yields were determined at 48 h p.i.

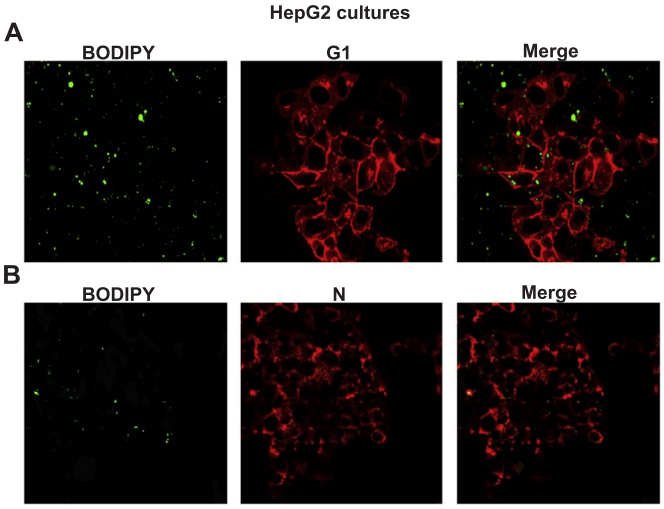


**Fig. 8. Subcellular localization of viperin and viral proteins.** HepG2 cultures were infected with JUNV and at 48 h p.i. cells were fixed, probed with BODIPY and stained with mouse monoclonal antibodies to reveal (A) JUNV G1 protein or (B) JUNV N protein. Magnification: 600×.

significantly induced the IFN-I pathway via a mechanism requiring RIG-I (Fig. 2). On the other hand, we showed that JUNV replication is hampered by IFN treatment. These findings seem to indicate that there is in fact an interplay between the virus and the cell immune response.

It is of our interest to determine the subcellular localization, intrinsic factors and specific time points for these viral-cell interactions which could be interfered for the benefit of the cell survival. In this line, physiologically relevant real time PCR assays and confocal microscopy studies were performed showing that endogenous viperin expression was specifically activated upon viral multiplication (Fig. 3). Then, we determined that viperin overexpression strongly reduced extracellular JUNV production in both, A549 and Vero IFN deficient cell cultures. Microscopy images showed that viperin overexpressing cultures were permissive to infection; however, a significant reduction in size of viral foci was observed. These results excluded the possibility that viperin is blocking virus entry, indicating another viral replication stage is being affected (Fig. 4), similar results have also been shown for the antiviral activity of viperin against tick-borne encephalitis virus (Upadhyay et al., 2014).

While investigating the mechanism by which viperin significantly reduces viral particle production, we detected alterations in cellular membrane G1 localization, which suggested an impairment of final morphogenesis or budding (Fig. 5). Although further studies are required, the overall viral glycoprotein mislocalization seen in viperin overexpressing cells would account for the JUNV antiviral viperin activity. These findings are in agreement with the negative modulation of particle release observed for human immunodeficiency (HIV) and Influenza viruses in viperin-overexpressing conditions. Reports have demonstrated that viperin is responsible for lipid rafts disturbance and, as a consequence, membrane localization of viral glycoproteins is impaired (Wang et al., 2007; Nasr et al., 2012). Since JUNV makes use of lipid rafts to bud from cells (Cordo et al., 2013), these lipid structures could be another possible link between viperin and its antiviral activity against JUNV.

On the other hand, altered lipogenesis has emerged as a common phenotype for pathological conditions like viral infections (Samsa et al., 2009; Seo and Cresswell, 2013). However, mechanisms that regulate LDs formation and how their function impacts in cellular biology remain unknown. Structurally and besides their rich lipid content, LDs contain several functionally diverse types of proteins, including already-described pro and antiviral relevant factors (Bozza et al., 1997; Yu et al., 2000; Fujimoto et al., 2001; Chen et al., 2002; Brasaemle et al., 2004; Liu et al., 2004; Wan et al., 2007; Pol et al., 2014). Therefore, lipid bodies might have potential implications for mechanisms of cell proliferation and differentiation, affecting viral replication.

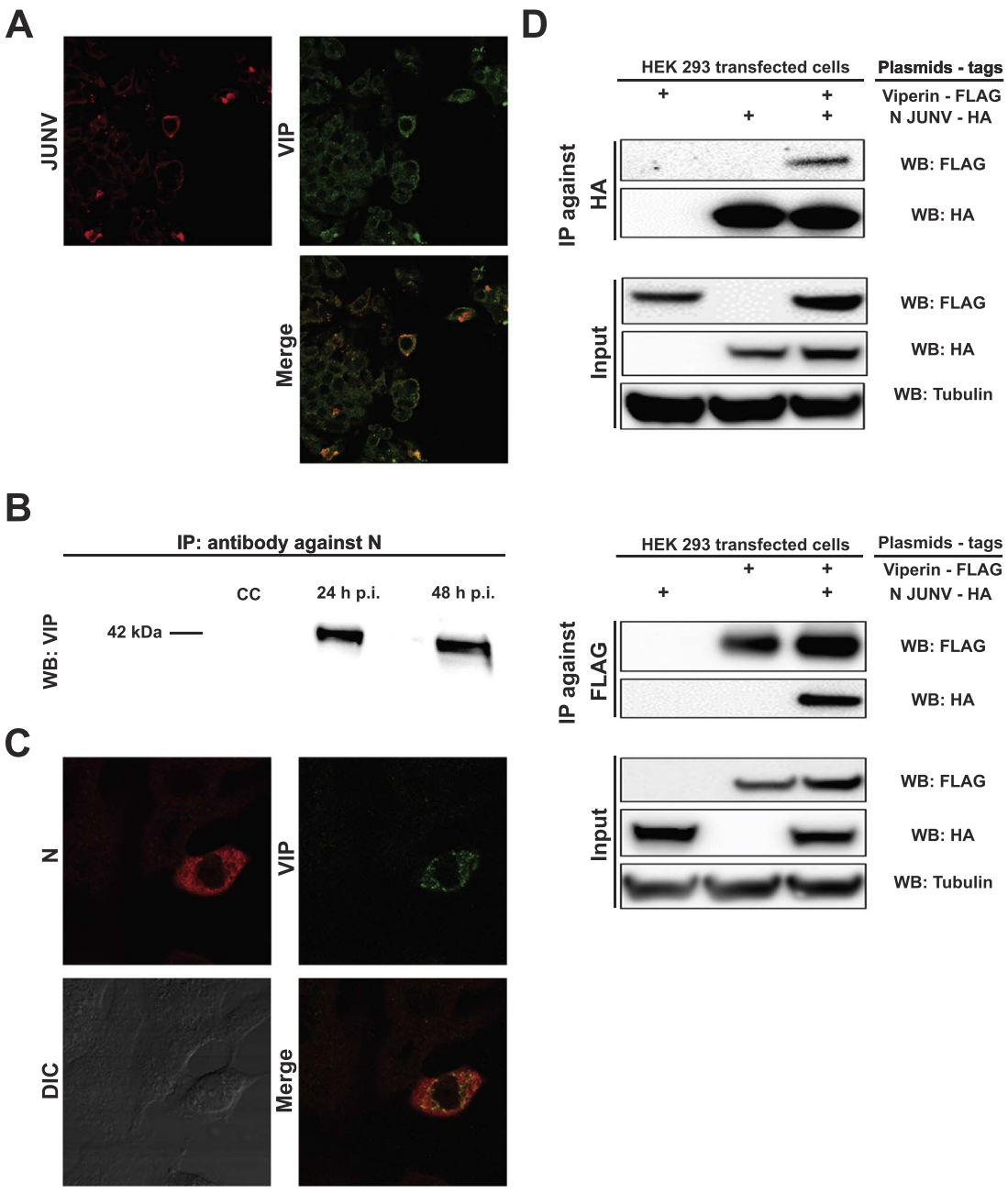


**Fig. 9. Interaction of viperin and JUNV N proteins.** (A) Infected HepG2 cells were stained with mouse monoclonal anti-viperin antibodies and rabbit polyclonal anti-JUNV antibodies, and further secondary antibodies incubation as detailed in Materials and methods. (B) A549 cells cultures were infected with JUNV at MOI of 0.1 PFU/cell. At 24 or 48 h p.i. monolayers were processed for immunoprecipitation anti-N (NA05AG12) antibodies. Immunocomplexes were subjected to WB analysis to detect viperin presence with polyclonal antibodies. As a control non infected cells (CC) collected with lysis buffer containing and processed as infected samples. (C) Co-localization of viperin- JUNV N protein. Representative image of co-transfected A549 cells stained with anti-viperin (green channel) and anti-N (red channel) antibodies. Merge panel shows co-localization overlap spots with a Pearson coefficient = 0.65. (D) HEK293T cells were transfected with plasmids encoding FLAG-tagged viperin and HA-tagged Junin N protein in different combinations as indicated (+). At 24 h p.t., cell extracts were subjected to anti-HA or anti-Flag immunoprecipitation. Whole cell lysate (input) and immunoprecipitated proteins were analyzed by immunobloting using antibodies as indicated. Tubulin served as a loading control. Representative images are shown from three independent experiments.

Recent studies have shown that mosquito derived cells accumulate and increase LD formation upon dengue infection (Barletta et al., 2016). These results together with those reported in human macrophages (Samsa et al., 2009), support the idea that these structures are important for virus multiplication. Interestingly, in this work we observed a decrease in LDs number in JUNV infected cells compare to non-infected cells (Fig. 6B and C). On the other hand, inhibiting lipid metabolism significantly reduced extracellular virus production (Fig. 7D). These observations demonstrate for the first time the importance of these lipid subcellular structures for proper JUNV replication. It was important to examine these particular lipid structures since viperin protein is reported to localize at this subcellular level. In addition, it was observed for the first time that N protein also localizes at LDs (Fig. 8B). This prompted us to investigate the possible N-viperin interaction through immunoprecipitation and confocal microscopy approaches. The protein-protein interaction was confirmed in both, cell infected and cell transfected samples (Fig. 9). Also, bioinformatic experimental approach was used to reveal protein interacting sites. According to predicted models from docking studies, the C-terminal of N protein would be involved in the interaction with α3 and α4 residues on viperin. Previous studies Zhang et al. (2013) determined that C-terminal domain of JUNV N (residues 341–564) might possess other

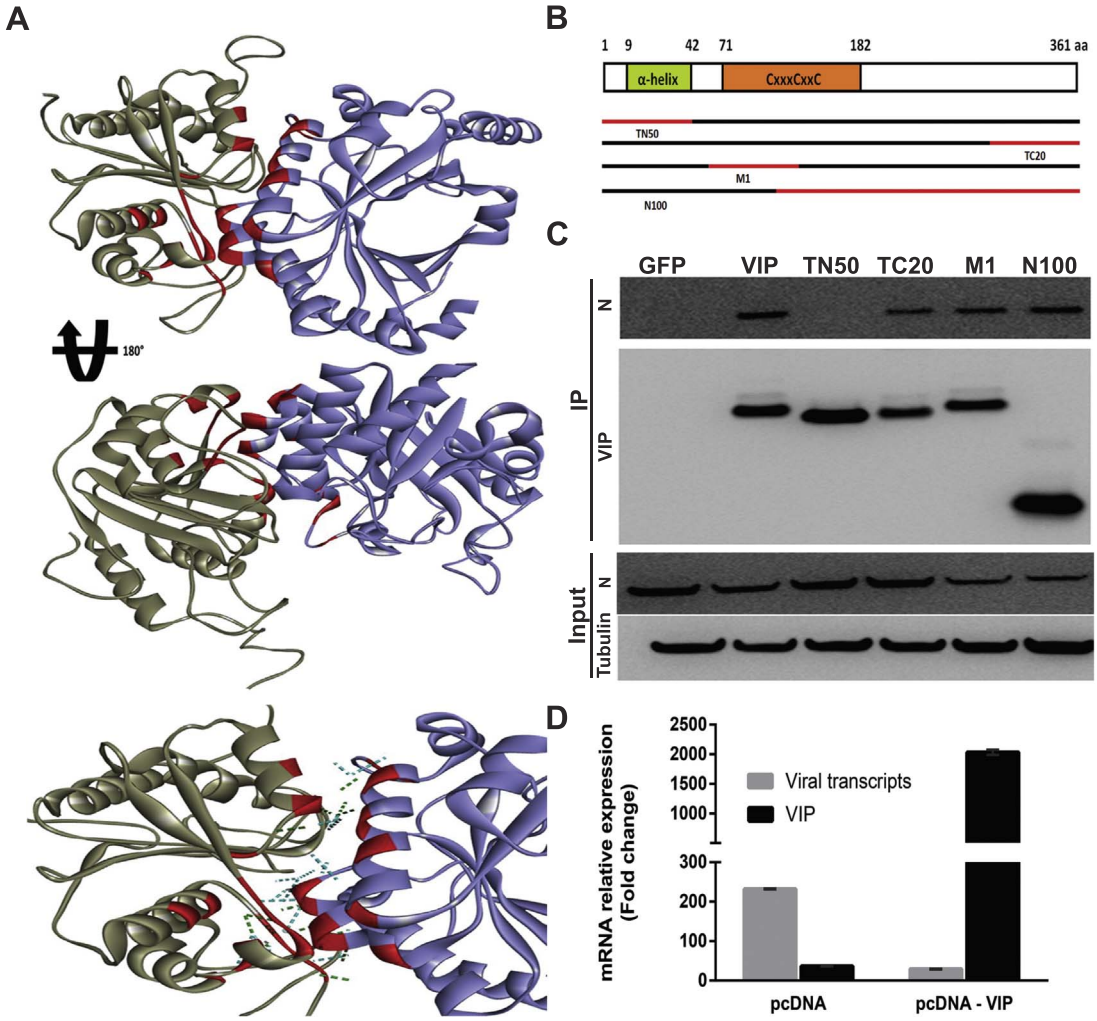


**Fig. 10. Mapping N-viperin interaction.** (A) Theoretical analysis of VIP- JUNV interaction. Ribbon schematic binding complex of viperin (blue) and JUNV N C-terminal domain (grey). Residues involved in interaction site are shown as red ribbon. Reverse view of the complex showing other interacting residues. Detailed projection of interacting residues of viperin-JUNV N complex. H-bonds are represented with green sticks and other electrostatic interactions are represented by cyan sticks. Both interactions were predicted using ClusPro and ZDock docking softwares. (B) Viperin mutants scheme. (C) HEK293T cells were transfected with plasmids encoding FLAG-tagged viperin mutants and HA-tagged Junin N protein in different combinations as indicated (+). At 24 h p.t., cell extracts were subjected to anti-Flag immunoprecipitation. Whole cell lysate (input) and immunoprecipitated proteins were analyzed by immunobloting using antibodies as indicated. Tubulin served as a loading control. Representative images are shown from three independent experiments. (D) Nucleoprotein functionality upon viperin expression. Both control and viperin transfected A549 cultures were infected at MOI of 0.1 PFU/cell. To determine viperin mRNA and viral transcription levels, monolayers were processed for real time PCR at 8 h p.i. Bars represent fold changes of mRNA relative expression in each condition compared to uninfected cell cultures.

important functions besides the exonuclease activity. Moreover, it has been indicated that amino acid residues between positions 394 and 502 (C-terminal of N) could be involved in zinc binding (Tortorici et al., 2001). On the other hand, viperin α3 belongs to the conserved central domain characteristic of *S*-adenosylmethionine (SAM) enzyme family (Shaveta et al., 2010) that has been implicated in HIV and Bunyamwera virus antiviral activity (Nasr et al., 2012; Carlton-Smith and Elliott, 2012). In this work, we could confirm using viperin mutants that at least the first 50 residues of viperin are required for the interaction (Fig. 10C). It is well known that the N-terminal targets viperin to lipid droplets (Hinson and Cresswell, 2009a), ER (Hinson and Cresswell, 2009b) and mitochondria (Seo et al., 2011), so N-viperin interaction might take place at these subcellular levels. Here, it was observed that N localizes to LD (Fig. 8B). Further studies need to be performed to gain more insight about other N subcellular localizations. Finally, further experiments are needed to determine the involvement of other viperin protein domains like C-terminal in the antiviral activity as it is crucial to flavivirus antiviral activity and interaction with other host cellular proteins (Helbig et al., 2013; Wang et al., 2012; Upadhyay et al., 2014, 2017; Van der Hoek et al., 2017). The arenaviral N is the most abundantly expressed viral protein in infected cells. N forms a ribonucleoprotein complex with the viral polymerase for the viral mRNAs transcription and synthesizes viral genomic RNAs during viral replication (Pinschewer et al., 2003). Interestingly, it was observed a significant inhibition in RNA transcription in viperin overexpressing-JUNV infected cell cultures, and cells depleted of viperin with siRNA showed higher viral transcripts (Fig. 10D). Our results suggest that JUNV RTC might be recruited to these lipid structures (Figs. 6B and 8B) and might use them as platforms for viral transcription, where viperin might interact with N in order to counteract this essential function. In addition, the findings that LDs downregulation has a negative impact on JUNV multiplication demonstrated for the first time that these structures are essential for arenavirus life cycle and might represent a novel antiviral target.

## 4. Conclusions

Restriction factors are considered the first line of defense against viruses. These antiviral proteins are synthesized at early times post infection, in host cellular environment to counteract viral replication. Altogether, our results report for the first time that viperin is an important restriction factor against JUNV infection with the final outcome

of limiting viral spread. Detailed mechanisms of action remain to be determined but several hints presented here suggest that viperin might act by two separately routes. Viral morphogenesis might be affected indirectly by negative modulation of lipid raft microdomains. Moreover, N ribonucleoprotein could be a direct target in trying to control viral replication as we found a significant inhibition in viral RNA transcription in viperin transfected-JUNV infected cells. Nevertheless, it cannot be discarded that other viral proteins could be also targeted by viperin protein. Further characterization should be done on the antiviral effect of viperin against JUNV and putative viperin-JUNV protein interactions remain to be studied.

The paradigm in which individual host cells could do nothing to prevent infection or interfere with downstream virus replication has changed a decade ago. The breakthrough discovery of cell-intrinsic restriction factors opened a new and interesting field in which the vulnerable points of the viral multiplication cycle could be attacked. Importantly, our results demonstrate that infected cells up-regulate viperin in trying to restrict JUNV replication. Although this naturally-occurring factor and others not yet characterized do not fully accomplish that goal, it is of great relevance to take them into account for the present understanding of the interplay between virus and host and for future antiviral therapy designs as well.

## 5. Materials and methods

### 5.1. Cells and viruses

A549 (human lung adenocarcinoma; ATCC CL-185), HepG2 (human hepatoma; ATCC CRL-10741) and Vero (African green monkey kidney; ATCC CCL 81) cell lines were grown in Eagle's minimum essential medium (MEM) (GIBCO) supplemented with 10%, 20% and 5% of fetal bovine serum respectively and 50 μg/ml gentamycin. HEK293T cells were grown in D-MEM. All cell lines were authenticated and tested for contamination. Virus stocks of JUNV (attenuated strain IV4454) were prepared and titrated by a standard plaque assay in Vero cells.

### 5.2. IFN treatment and viperin induction

A549 or Vero cells were treated for 8 h with 10,000 IU/ml of IFN-α (Bioferon, Argentina), infected with JUNV at a MOI of 0.1 PFU/cell, or alternatively pretreated for 8 h with 10,000 IU/ml of IFN-α and then infected with JUNV at a MOI of 0.1 PFU/cell. At different times post treatment or infection; cells were fixed or lysed and processed for immunofluorescence or real time PCR assay, respectively. Cell viability in the presence of different concentrations of IFN-α was determined by methylthiazolyldiphenyl-tetrazolium bromide (MTT; Sigma-Aldrich) method (Berridge et al., 2005).

### 5.3. Real time RT-PCR assay

Total RNA was extracted using TRIZOL (Invitrogen Life Technologies) according to manufacturer's instructions. Then, cDNA was generated by use of murine reverse transcriptase M-MLV (Promega) and random primers (Biodynamics, Argentina). This cDNA was amplified by real time PCR using SYBRGreen complete mix detection (Biodynamics, Argentina). Real time PCR was carried out with an initial incubation at 95 °C during 2 min, followed by 35 cycles of 30 s at 95 °C, 1 min at 58 °C, and 1 min at 72 °C and a final step of 10 min at 72 °C. Amplification plots were analyzed with Biorad software and the comparative threshold cycle method was used to determine gene expression relative to β-actin cellular gene. Primer sequences are detailed in Giovannoni et al. (2015). Results are expressed as the mean ± SD of 2 independent experiments.

### 5.4. Plasmid and siRNAs transfections

Viperin encoding plasmid (pcDNA3.1-VIP) was kindly provided by Dr. Peter Cresswell (Yale University, New Haven, CT, USA). Viperin mutant encoding plasmids were described in (Wang et al., 2012; Upadhyay et al., 2014). The N-terminally FLAG-tagged N100 viperin (1–100 aa) was constructed based on the eukaryotic expression vector pI.18 (kindly provided by Jim Robertson, National Institute for Biological Standards and Control, Hertfordshire, United Kingdom), using standard PCR cloning methods. KOD Hot Start polymerase (Novagen), restriction enzymes and T4 DNA ligase (Fermentas) were used according to the manufacturers' recommendations. The plasmid was sequenced to ensure correctness, and oligonucleotide primer sequences are available upon request.

JUNV-N encoding plasmid (pcDNA3.1-N) was previously generated in our lab (Artuso et al., 2009). Plasmid (1 μg/ml) was transfected into A549 cells using Lipofectamine 2000 (Invitrogen Life Technologies). For viperin silencing assay 100 nM of commercial siRNAs (sc-94261 RSAD2 siRNA (h), Santa Cruz Biotechnology) were transfected into A549 cells. Sequence of RNA used as control was 5′-GACCACAATTCT CGATATACAUU-3′. Cells were infected with JUNV at a MOI of 0.1 PFU/cell at 24 h p.t. At 24 h p.i., extracellular medium was harvested to quantify virus production and cells were processed for immunofluorescence or real time PCR assays.

### 5.5. Indirect immunofluorescence (IF) assay

For cytoplasmic IF, cells were grown on coverslips and fixed by incubation in 4% paraformaldehyde for 15 min at room temperature, washed three times with PBS and finally permeabilized by incubation in 0.1% Triton X-100 in PBS for 15 min at room temperature. Fixed cells were rinsed three times with PBS before incubation in blocking buffer (3% BSA, 0.15% Triton X-100 in PBS) for 1 h at 37 °C. For viperin detection, indirect staining was carried out by incubating with 1/50 dilution of rabbit polyclonal (sc-102099 RSAD2, Santa Cruz Biotechnology) or 1/100 dilution of mouse monoclonal anti-viperin antibodies (MaPVip, kindly provided by Dr. Peter Cresswell) for 1 h at 37 °C, followed by a second incubation with 1/100 dilution of Alexa 488 conjugated goat anti- rabbit or mouse IgG antibodies, respectively. LD associated protein perilipin 2 (Plin2) detection was performed by using guinea pig antibodies (2OR-APOO2, Fitzgerald; kindly provided by Dr. Andrea Gamarnik) at 1/100 dilution, overnight (ON) at 4 °C. Then, anti-guinea pig-FITC was used at 1/300 dilution for 1 h at 37 °C. For viral proteins, indirect staining was carried out by incubating with 1/300 dilution of mouse monoclonal anti-G1 (GB03BE08) or anti-N (NA05AG12) antibodies (Sanchez et al., 1989) and 1/100 dilution of Alexa 568-conjugated goat anti-mouse IgG antibodies. Alternatively, 1/50 dilution of rabbit polyclonal anti-JUNV antibodies generated in our laboratory was used. After a final washing with PBS, cells were stained with 4′,6-diamidino-2-phenylindole dihydrochloride (DAPI) and mounted. For specific membrane IF, cells were first washed with ice-cold PBS and then incubated with mouse monoclonal anti-G1 antibodies or anti-viperin antibodies at 37 °C for 60 min. After washing with cold PBS, cells were fixed for 15 min in 4% paraformaldehyde at 37 °C and further incubated with Alexa 568 or 488 conjugated antibodies, respectively. Mounted cells were visualized and images were acquired using an Olympus IX71 microscope or a confocal Olympus Fluoview FV300.

### 5.6. Quantification of G1 positive cells and viral foci

Total cells were counted on 3 different images from 3 different fields randomly chosen. Quantifications of DAPI stained nucleus were performed through setting the right threshold followed by automatic particle analysis in Fiji. Cells going under division (segmented nucleus or visible chromosomes) were discarded. G1 viral antigen expressing cells

were considered positive under two criteria: 1) rounded morphology of the cell (infected cells become rounded as a result of the cytopathic effect) and 2) perinuclear expression pattern of G1. Manual counting was made through the cell counter plugin of Fiji. Percentage of G1 positive cells was expressed as the ratio between G1 positive cells and total cells in each field and then the average percentage was determined and presented. Viral foci were delimited considering groups of G1 positive cells surrounded by G1 negative cells. Viral foci were counted on 3 different images from 3 different fields chosen randomly and the average foci size was determined by the number of cells that formed them. An unpaired student t- test was performed between infected-transfected cells with empty vector and viperin encoding vector.

### 5.7. Lipid droplet staining and counting

For LD staining HepG2 cells were fixed and then incubated with 1 μM of BODIPY 493/503 (Molecular Probes) for 10 min, which allows fluorescent detection of LDs. Photographs were taken using an Olympus IX71 epifluorescence microscope. For samples stained with Plin2 antibodies, IF protocol was carried as in section 4.5. Photographs were taken using a confocal Olympus Fluoview FV300 confocal microscope.

LDs probed with BODIPY, were automatically quantified using Fiji program by differentiation of background from the particles of interest. A binary mask was made setting a default threshold of 73–255 minimum and maximum intensities respectively that allowed selecting LDs. This binary image was subtracted from the original one and resulting image showed LDs without background. This image was thresholded again for a better and more specific selection of particles with values of 89–255 minimum and maximum. Then, values of size between 0.002-infinity and circularity between 0.7 and 1.00 were set. For Plin2 stained LDs a maximum intensity projection of each stack was created for the red, green and brightfield channels. For counting, a division between two populations of cells was made: those positive and negative for JUNV N staining were considered infected and not infected, respectively. Finally, the number of LD was determined for each cell following the steps detailed for BODIPY stained samples, with thresholds determined accordingly.

### 5.8. C75 Inhibitor assays

Cell viability in the presence of C75 (Sigma-Aldrich) was determined by MTT method as described before in section 4.2 and by crystal violet dye method (Feoktistova et al., 2016). To evaluate the effect of C75 on LDcontent, HepG2 cultures were incubated with 23 μM of C75, fixed, stained and quantified by BODIPY staining as detailed in section 4.7. For inactivation assay, equal volumes of viral suspension containing $1 \times 10^6$PFU/ml and various concentrations of C75 were mixed and incubated at 37 °C for 90 min. Then, dilutions of the different mixtures were made and titrated in Vero cells by standard plaque assay. As a control, viral suspension was incubated under the same conditions with a similar volume of dimethyl sulfoxide. To evaluate C75 effect upon JUNV replication, cells were infected, treated with different C75 concentrations and at 48 h p.i. supernatants were harvested and quantified by plaque assay. Percentage of the remaining infectivity relative to viral control was determined. For all experiments, ANOVA of one factor was performed, followed by a Tukey test.

### 5.9. JUNV-viperin interaction assays

#### 5.9.1. Immunoprecipitation assay

A549 cells cultures were infected with JUNV at MOI of 0.1 PFU/cell. At 24 or 48 h p.i. monolayers were washed with PBS and collected using lysis buffer (TBS containing 1% CHAPS, 0,4 mM PMSF, 3,5 μg/ml pepstatin). After three steps of freeze and unfreeze, cells were centrifuged and supernatants were incubated with anti-N (NA05AG12) antibodies, following incubation with agarose- protein A, for 30 min at 37 °C under continuous shaking and 90 min at 4 °C. After centrifugation, pellet was washed three times with lysis buffer. Immunocomplexes were resuspended in SDS-PAGE with β-mercaptoethanol and incubated at 100 °C for 5 min. Supernatants were collected for WB assays (12% polyacrilamide gel) to detect viperin presence with polyclonal antibodies. As a control non infected cells were processed as infected samples. Immunoprecipitation of FLAG or HA-tagged proteins was performed as previously described (Wang et al., 2012; Upadhyay et al., 2014) using the following antibodies: mouse anti-FLAG epitope (200472, Stratagene) and rabbit anti-FLAG epitope (F7425, Sigma), were used at 1/5000 dilution; mouse anti-HA epitope (ab18181, Abcam) and rabbit anti-HA epitope (ab9110, Abcam) were used at 1/4000 dilution; rabbit anti- tubulin (ab6046, Abcam) was used at 1/4000 dilution. Horseradish peroxidase-conjugated secondary antibody was obtained from Pierce and antigen detection was performed using Supersignal West Pico or Femto kit (Pierce).

#### 5.9.2. Co-localization studies

A549 cell cultures were co-transfected with pcDNA3.1-VIP and pcDNA3.1-N plasmids according to section 4.4. At 24 h p.t., cultures were fixed for IFI and stained with the corresponding antibodies. Immunolocalization of viperin and N was analyzed by confocal Olympus Fluoview FV300 microscope in cells co-expressing the proteins. Pearson coefficient was calculated to determine co-localization (Manders et al., 1993).

#### 5.9.3. Computational studies

The structure of JUNV N protein was retrieved from Protein Data Bank (PDB, ID: 4K7E) (Zhang et al., 2013). It is the crystal structure of the C-terminal domain (residues 341–564) with 2.2 Å resolution. Missing residues were added by Chimera software (Pettersen et al., 2004). The crystal structure with 1.7 Å resolution of viperin protein was also retrieved from PDB (ID:5VSM) (Fenwick et al., 2017). Viperin was docked into N protein utilizing two different protein-protein docking softwares, ClusPro (Comeau et al., 2004) and ZDock (Pierce et al., 2014), in a comparative manner. These programs produced different complex models and the most common viperin–N interaction model was selected.

#### 5.9.4. Viral transcription assay

A549 cell cultures were transfected with pcDNA3.1-VIP encoding plasmid and at 24 h p.t cells were infected at a MOI of 0.1 PFU/cell. At 24 h p.i., total RNA was extracted, cDNA was generated and specific viral RNA transcripts and viperin mRNAs were amplified by real time PCR using appropriate primers. For viral transcripts: sense 5′-GGCAT CCTTCAGAACAT-3′ and antisense 5′-CGCACAGTGGATCCTAGGC-3′ primers were used to generate a 186 bp amplification fragment comprising the 3′ end of the S RNA containing N coding sequences. For viperin amplification, sense 5′-CGTGGAAGAGGACATGACGGAAC-3′ and antisense 5′-CCGCTCTACCAAATCCAGCTTC-3′ were used. Amplification plots were analyzed with Biorad software and the comparative threshold cycle method was used to determine gene expression relative to control cultures β-actin gene.

### 5.10. Statistical analysis

All data were analyzed by InfoStat, a free software available to download from http://www.infostat.com.ar. Data shown are result of independent experiments and error bars from graphics represent SD. All data were tested for normal distribution using the Shapiro-Wilks test before applying further statistical analysis. Comparisons of 2 data sets were performed by an unpaired t-student test while comparison between 3 or more data sets was performed by an analysis of variance (ANOVA) for a single factor. A p value $< 0.05$ was the criteria met for considering significant differences (marked as asterisks in the graphics) and when obtained in ANOVA, a Tukey post-hoc comparison test was

performed in order to know between which groups the differences were.

### 5.11. Graphics and image processing

All graphics were made in GraphPad Prism 6.00 software, image processing and analysis was made using Fiji software. Both are free software (http://graphpad.com/demos/ and http://fiji.sc/Downloads).

## Acknowledgements

We acknowledge Dr. Peter Cresswell (Yale University, New Haven, CT, USA) for helpful discussions and reagents.

## Competing interests

The authors declare no conflict of interest.

## Author contributions

Conceived and designed the experiments: J.R.P.C, M.L.M, S.V, A.S.U, A.K.O, S.M.C, C.C.G. Performed the experiments: J.R.P.C, M.L.M, C.A.V, S.V, A.K.U. Analyzed the data: J.R.P.C, M.L.M, C.A.V, S.V, A.S.U, A.K.O, S.M.C, C.C.G. Designed and assembled figures: M.L.M, A.S.U, A.K.O, S.M.C, C.C.G. Contributed reagents/materials/analysis tools: A.K.O, S.M.C, C.C.G. Wrote the paper: S.M.C, C.C.G. All authors read and approved the final manuscript.

## Funding

This study was supported by Universidad de Buenos Aires (UBA) (20020120100033), Consejo Nacional de Investigaciones Científicas y Tecnológicas (CONICET) (PIP-0293) and Agencia de Promoción Científica y Tecnológica (ANPCyT) (BID-PICT 517). S.M.C and C.C.G are members of the Research Career CONICET, J.R.P.C and C.A.V are CONICET fellows and M.L.M is a doctoral fellow of UBA. J.R.P.C has received funds from The Company of Biologists Limited-Travelling Fellowships Program.

## References

Artuso, M.C., Ellenberg, P.C., Scolaro, L.A., Damonte, E.B., García, C.C., 2009. Inhibition of Junin virus replication by small interfering RNAs. Antivir. Res. 84 (1), 31–37.
Barletta, A.B., Alves, L.R., Nascimento Silva, M.C., Sim, S., Dimopoulos, G., Liechocki, S., Maya-Monteiro, C.M., Sorgine, M.H., 2016. Emerging role of lipid droplets in *Aedesaegypti* immune response against bacteria and Dengue virus. Sci. Rep. 6, 19928.
Berridge, M.V., Herst, P.M., Tan, A.S., 2005. Tetrazolium dyes as tools in cell biology: new insights into their cellular reduction. Biotechnol. Annu. Rev. 11, 127–152.
Bozza, P.T., Yu, W., Penrose, J.F., Morgan, E.S., Dvorak, A.M., Weller, P.F., 1997. Eosinophil lipid bodies: specific, inducible intracellular sites for enhanced eicosanoid formation. J. Exp. Med. 186, 909–920.
Brasaemle, D.L., Dolios, G., Shapiro, L., Wang, R., 2004. Proteomic analysis of proteins associated with lipid droplets of basal and lipolytically stimulated 3T3-L1 adipocytes. J. Biol. Chem. 279, 46835–46842.
Carlton-Smith, C., Elliott, R.M., 2012. Viperin, MTAP44, and protein kinase R contribute to the interferon-induced inhibition of Bunyamwera Orthobunyavirus replication. J. Virol. 86, 11548–11557.
Chen, J.S., Greenberg, A.S., Wang, S.M., 2002. Oleic acid-induced PKC isozyme translocation in RAW 264.7 macrophages. J. Cell Biochem. 86, 784–791.
Chin, K.C., Cresswell, P., 2001. Viperin (cig5), an IFN-inducible antiviral protein directly induced by human cytomegalovirus. Proc. Natl. Acad. Sci. USA 98, 15125–15130.
Comeau, S.R., Gatchell, D.W., Vajda, S., Camacho, C.J., 2004. ClusPro: an automated docking and discrimination method for the prediction of protein complexes. Bioinformatics 20, 45–50.
Cordo, S.M., Candurra, N.A., Damonte, E.B., 1999. Myristic acid analogs are inhibitors of Junin virus replication. Microbes Infect. 8, 609–614.
Cordo, S.M., Valko, A., Martinez, G.M., Candurra, N.A., 2013. Membrane localization of Junín virus glycoproteins requires cholesterol and cholesterol rich membranes. Biochem. Biophys. Res. Commun. 430, 912–917.
Eichler, R., Lenz, O., Strecker, T., Eickman, M., Klenk, H.D., Garten, W., 2003. Identification of Lassa virus glycoprotein signal peptide as a trans-acting maturation factor. EMBO Rep. 4, 1084–1088.
Enria, D.A., Briggiler, A.M., Sánchez, Z., 2008. Treatment of Argentine hemorrhagic fever. Antivir. Res. 78, 132–139.
Fan, L., Briese, T., Lipkin, W.I., 2010. Z proteins of New World arenaviruses bind RIG-I and interfere with type I interferon induction. J. Virol. 84, 1785–1791.
Fenwick, M.K., Li, Y., Cresswell, P., Modis, Y., Ealick, S.E., 2017. Structural studies of viperin, an antiviral radical SAM enzyme. Proc. Natl. Acad. Sci. USA 114, 6806–6811.
Feoktistova, M., Geserick, P., Leverkus, M., 2016. Crystal violet assay for determining viability of cultured cells. Cold Spring Harb. Protoc.(4) (pdb.prot087379).
Fujimoto, T., Kogo, H., Ishiguro, K., Tauchi, K., Nomura, R., 2001. Caveolin-2 is targeted to lipid droplets, a new "membrane domain" in the cell. J. Cell Biol. 152, 1079–1085.
García, C.C., Ellenberg, P.C., Artuso, M.C., Scolaro, L.A., Damonte, E.B., 2009. Characterization of Junín virus particles inactivated by a zinc finger-reactive compound. Virus Res. 143 (1), 106–113.
Gaudin, R., Barteneva, N.S., 2015. Sorting of small infectious virus particles by flow virometry reveals distinct infectivity profiles. Nat. Commun. 6, 6022.
Giovannoni, F., Damonte, E.B., García, C.C., 2015. Cellular promyelocytic leukemia protein is an important dengue virus restriction factor. PLoS One 10 (5), e0125690.
Groseth, A., Hoenen, T., Weber, M., Wolff, S., Herwig, A., Kaufmann, A., Becker, S., 2011. Tacaribe virus but not junin virus infection induces cytokine release from primary human monocytes and macrophages. PLoS Negl. Trop. Dis. 5 (5), e1137.
Helbig, K.J., Beard, M.R., 2014. The role of viperin in the innate antiviral response. J. Mol. Biol. 426 (6), 1210–1219.
Helbig, K.J., Carr, J.M., Calvert, J.K., Wati, S., Clarke, J.N., Eyre, N.S., Narayana, S.K., Fiches, G.N., McCartney, E.M., Beard, M.R., 2013. Viperin is induced following dengue virus type-2 (DENV-2) infection and has anti-viral actions requiring the C-terminal end of viperin. PLoS Negl. Trop. Dis. 18 (4), e2178 (7).
Hinson, E.R., Cresswell, P., 2009a. The antiviral protein, viperin, localizes to lipid droplets via its N-terminal amphipathic alpha-helix. Proc. Natl. Acad. Sci. Usa. 106, 20452–20457.
Hinson, E.R., Cresswell, P., 2009b. The N-terminal amphipathic alpha-helix of viperin mediates localization to the cytosolic face of the endoplasmic reticulum and inhibits protein secretion. J. Biol. Chem. 284, 4705–4712.
Hinson, E.R., Joshi, N.S., Chen, J.H., Rahner, C., Jung, Y.W., Wang, X., Kaech, S.M., Cresswell, P., 2010. Viperin is highly induced in neutrophils and macrophages during acute and chronic lymphocytic choriomeningitis virus infection. J. Immunol. 184 (10), 5723–5731.
Huang, C., Kolokoltsova, O.A., Yun, N.E., Seregin, A.V., Poussard, A.L., Walker, A.G., Brasier, A.R., Zhao, Y., Tian, B., de la Torre, J.C., Paessler, S., 2012. Junín Virus Infection Activates the Type I Interferon Pathway in a RIG-I-Dependent Manner. PLoS Negl. Trop. Dis. 6 (5), e1659.
Huang, C., Walker, A.G., Grant, A.M., Kolokoltsova, O.A., Yun, N.E., Seregin, A.V., Paessler, S., 2014. Potent inhibition of Junín virus infection by interferon in murine cells. PLoS Negl. Trop. Dis. 8, e2933.
Huang, C., Kolokoltsova, O.A., Yun, N.E., Seregin, A.V., Ronca, S., Koma, T., Paessler, S., 2015. Highly pathogenic new world and old world human arenaviruses induce distinct interferon responses in human cells. J. Virol. 89, 7079–7088.
Jiang, X., Chen, Z.J., 2011. Viperin links lipid bodies to immune defense. Immunity 34, 285–287.
Kluge, S.F., Sauter, D., Kirchoff, F., 2015. SnapShot: antiviral restriction factors. Cell 163 (774-774).
Kuhajda, F.P., Landree, L.E., Ronnett, G.V., 2005. The connections between C75 and obesity drug-target pathways. Trends Pharmacol. Sci. 26, 541–544.
Levis, S.C., Saavedra, M.C., Ceccoli, C., Falcoff, E., Feuillade, M.R., Enria, D.A., Maiztegui, J.I., Falcoff, R., 1984. Endogenous interferon in Argentine hemorrhagic fever. J. Infect. Dis. 149 (3), 428–433.
Liu, P., Ying, Y., Zhao, Y., Mundy, D.I., Zhu, M., Anderson, R.G., 2004. Chinese hamster ovary K2 cell lipid droplets appear to be metabolic organelles involved in membrane traffic. J. Biol. Chem. 279, 3787–3792.
Loftus, T.M., Jaworsky, D.E., Frehywot, G.L., Townsend, C.A., Ronnett, G.V., Lane, L.D., Kuhajda, F.P., 2000. Reduced food intake and body weight in mice treated with fatty acid synthase inhibitors. Science 288, 2379–2381.
Makins, C., Ghosh, S., Román-Meléndez, G.D., Malec, P.A., Kennedy, R.T., Marsh, E.N., 2016. Does viperin function as a radical S-Adenosyl-L-methionine-dependent enzyme in regulating farnesylpyrophosphate synthase expression and activity? J. Biol. Chem. 291, 26806–26815.
Manders, E.M., Verbeek, F.J., Aten, J.A., 1993. Measurement of co-localization of objects in dual-colour confocal images. J. Microsc. 169, 375–382.
Martínez-Sobrido, L., Zúñiga, E.I., Rosario, D., García-Sastre, A., de la Torre, J.C., 2006. Inhibition of the type I interferon response by the nucleoprotein of the prototypic arenavirus lymphocytic choriomeningitis virus. J. Virol. 80, 9192–9199.
McGillivary, G., Jordan, Z.B., Peeples, M.E., Bakaletz, L.O., 2013. Replication of respiratory syncytial virus is inhibited by the host defense molecule viperin. J. Innate Immun. 5, 60–71.
Nasr, N., Maddocks, S., Turville, S.G., Harman, A.N., Woolger, N., Helbig, K.J., Wilkinson, J., Bye, C.R., Wright, T.K., Rambukwelle, D., Donaghy, H., Beard, M.R., Cunningham, A.L., 2012. HIV-1 infection of human macrophages directly induces viperin which inhibits viral production. Blood 120, 778–788.
Paessler, S., Walker, D.H., 2013. Pathogenesis of the viral hemorrhagic fevers. Annu. Rev. Pathol. 8, 411–440.
Pettersen, E.F., Goddard, T.D., Huang, C.C., Couch, G.S., Greenblatt, D.M., Meng, E.C., Ferrin, T.E., 2004. UCSF Chimera a visualization system for exploratory research and analysis. J. Comput. Chem. 25, 1605–1612.
Pierce, B.G., Wiehe, K., Hwang, H., Kim, B.H., Vreven, T., Weng, Z., 2014. ZDock server: interactive docking prediction of protein-protein complexes and symmetric multimers. Bioinformatics 30, 1771–1773.
Pinschewer, D.D., Perez, M., de la Torre, J.C., 2003. Role of the virus nucleoprotein in the regulation of lymphocytic choriomeningitis virus transcription and RNA replication.

J. Virol. 77 (6), 3882–3887.
Pol, A., Gross, S.P., Parton, R., 2014. Review: biogenesis of the multifunctional lipid droplet: lipids, proteins, and sites. J. Cell Biol. 204, 635–646.
Pythoud, C., Rothenberger, S., Martínez-Sobrido, L., de la Torre, J.C., Kunz, S., 2015. Lymphocytic Choriomeningitis virus differentially affects the virus-induced type I Interferon response and mitochondrial apoptosis mediated by RIG-I/MAVS. J. Virol. 89, 6240–6250.
Radoshitzky, S.R., Bào, Y., Buchmeier, M.J., Charrel, R.N., Clawson, A.N., Clegg, C.S., DeRisi, J.L., Emonet, S., Gonzalez, J.P., Kuhn, J.H., Lukashevich, I.S., Peters, C.J., Romanowski, V., Salvato, M.S., Stenglein, M.D., de la Torre, J.C., 2015. Past, present, and future of arenavirus taxonomy. Arch. Virol. 160, 1851–1874.
Ronnett, G.V., Kim, E.K., Landree, L.E., Tu, Y., 2005. Fatty acid metabolism as a target for obesity treatment. Physiol. Behav. 85, 25–35.
Saka, H.A., Valdivia, R., 2012. Emerging roles for lipid droplets in immunity and host-pathogen interactions. Annu. Rev. Cell Dev. Biol. 28, 411–437.
Samsa, M.M., Mondotte, J.A., Iglesias, N.G., Assunção-Miranda, I., Barbosa-Lima, G., Da Poian, A.T., Bozza, P.T., Gamarnik, A.V., 2009. Dengue virus capsid protein usurps lipid droplets for viral particle formation. PLoS Pathog. 5 (10), e1000632.
Sanchez, A., Pifat, D.Y., Kenyon, R.H., Peters, C.J., McCormick, J.B., Kiley, M.P., 1989. Junin virus monoclonal antibodies: characterization and cross-reactivity with other arenaviruses. J. Gen. Virol. 70, 1125–1132.
Seo, J.Y., Cresswell, P., 2013. Viperin regulates cellular lipid metabolism during human cytomegalovirus infection. PLoS Pathog. 9 (8), e1003497.
Seo, J.Y., Yaneva, R., Cresswell, P., 2011. Viperin: a multifunctional, interferon-inducible protein that regulates virus replication. Cell Host Microbe 10 (6), 534–539.
Shaveta, G., Shi, J., Chow, V.T., Song, J., 2010. Structural characterization reveals that viperin is a S-adenosyl-L-methionine (SAM) enzyme. Biochem. Biophys. Res. Commun. 391, 1390–1395.
Tan, K.S., Olfat, F., Phoon, M.C., Hsu, J.P., Howe, J.L., Seet, J.E., Chin, K.C., Chow, V.T., 2012. In vivo and in vitro studies on the antiviral activities of viperin against influenza H1N1 virus infection. J. Gen. Virol. 93, 1269–1277.
Teng, T.S., Foo, S.S., Simamarta, D., Lum, F.M., Teo, T.H., Lulla, A., Yeo, N.K., Koh, E.G., Chow, A., Leo, Y.S., Merits, A., Chin, K.C., Ng, L.F., 2012. Viperin restricts chikungunya virus replication and pathology. J. Clin. Investig. 122, 4447–4460.
Tortorici, M.A., Ghiringhelli, P.D., Lozano, M.E., Albarino, C.G., Romanowski, V., 2001. Zinc-binding properties of Junín virus nucleocapsid protein. J. Gen. Virol. 82, 121–128.
Upadhyay, A.S., Vonderstein, K., Pichlmair, A., Stehling, O., Bennett, K.L., Dobler, G., Guo, J.T., Superti-Furga, G., Lill, R., Överby, A.K., Weber, F., 2014. Viperin is an iron-sulfur protein that inhibits genome synthesis of tick-borne encephalitis virus via radical SAM domain activity. Cell Microbiol. 16, 834–848.
Upadhyay, A.S., Stehling, O., Panayiotou, C., Rösser, R., Lill, R., Överby, A.K., 2017. Cellular requirements for iron-sulfur cluster insertion into the antiviral radical SAM protein viperin. J. Biol. Chem. 292, 13879–13889.
Van der Hoek, K.H., Eyre, N.S., Shue, B., Khantisitthiporn, O., Glab-Ampi, K., Carr, J.M., Gartner, M.J., Jolly, L.A., Thomas, P.Q., Adikusuma, F., Jankovic-Karasoulos, T., Roberts, C.T., Helbig, K.J., Beard, M.R., 2017. Viperin is an important host restriction factor in control of Zika virus infection. Sci. Rep. 7, 4475.
Wan, H.C., Melo, R.C., Jin, Z., Dvorak, A.M., Weller, P.F., 2007. Roles and origins of leukocyte lipid bodies: proteomic and ultrastructural studies. FASEB J. 21, 167–178.
Wang, H., Quiroga, A.D., Lehner, R., 2013. Analysis of lipid droplets in hepatocytes. Methods Cell Biol. 116, 107–127.
Wang, S., Wu, X., Pan, T., Song, W., Wang, Y., Zhang, F., Yuan, Z., 2012. Viperin inhibits hepatitis C virus replication by interfering with binding of NS5A to host protein hVAP-33. J. Gen. Virol. 93, 83–92.
Wang, X., Hinson, E.R., Creswell, P., 2007. The interferon-inducible protein viperin inhibits influenza virus release by perturbing lipid rafts. Cell Host Microbe 2, 96–105.
Xing, J., Ly, H., Liang, Y., 2015. The Z proteins of pathogenic but not nonpathogenic arenaviruses inhibit RIG-I-like receptor-dependent interferon production. J. Virol. 89, 2944–2955.
York, J., Romanowski, V., Lu, M., Nunberg, J.H., 2004. The signal peptide of the Junín arenavirus envelope glycoprotein is myristoylated and forms an essential subunit of the mature G1-G2 complex. J. Virol. 78, 10783–10792.
Yu, W., Cassara, J., Weller, P.J., 2000. Phosphatidylinositide 3-kinase localizes to cytoplasmic lipid bodies in human polymorphonuclear leukocytes and other myeloid-derived cells. Blood 95, 1078–1085.
Zhang, Y., Li, L., Liu, X., Dong, S., Wang, W., Huo, T., Guo, Y., Rao, Z., Yang, C., 2013. Crystal structure of Junin virus nucleoprotein. J. Gen. Virol. 94, 2175–2183.